WETTABILITY EVALUATION OF SUPER WETTING SURFACES COATED WITH NANOPARTICLES

Erivelto dos Santos Filho, Térmica e Fluidos, erivelto.usp@gmail.com
Francisco Júlio do Nascimento, Térmica e Fluidos, fnascimento@sc.usp.br
Debora Carneiro Moreira, Térmica e Fluidos, dcmoreira@id.uff.br
Gherhardt Ribatski, Térmica e Fluidos, ribatski@sc.usp.br

Abstract. *The present study concerns an investigation on the variation of wettability and roughness of a flat aluminun plate covered with a porous thin-film of nanoparticles. The contact angle of surfaces covered with a film of nanoparticles is almost null; hence, conventional methods are not suitable to evaluate the contact angle under this condition. Therefore, in the present study a new method was developed to evaluate the wettability. This method is based on the spreading velocity of a water droplet deposited on the surface. Aluminum oxide 20-30nm and 40-80nm nanoparticles were deposited on aluminum plates through a nucleate boiling process. The depositions were obtained through pool boiling of water/Al_2O_3 nanofluids containing 0.01%, 0.1% and 0.5% in volume of nanoparticles. The roughness parameter Rt (maximum distance from peak to valley) increases with increasing volumetric concentration of the boiled nanofluid for aluminum oxide 20-30nm and decrease for 40-80nm. Based on the wettability reuslts, two spreading mechanisms were identified, which are probably related to inertial and capillarity effects. In addition, it was noticed that droplet spreading velocity on surfaces covered with aluminum oxide 20-30nm for all concentrations and for aluminum oxide 40-80nm 0.5% is nearly the same, while surfaces covered with Al_2O_3 40-80nm for 0.01% and 0.1% shown higher spreading velocity.*

Keywords: Nanofluid, Nanoparticle, Roughness, Wettability, Critical Heat Flux.

1. INTRODUCTION

Several important industrial applications rely on nucleate boiling to remove high heat fluxes from heated surfaces: nuclear reactors, chemical reactors, electronic devices and solar power absorbers. Nucleate boiling is an effective mode to remove high heat flux, it can dissipate heat fluxes up to two orders of magnitude larger than single-phase heat transfer for a given temperature difference (Nikolayev et al., 2006). The efficiency of the heater exchanger increases with increasing heat flux for the same wall superheating. However, there is a limit called critical heat flux (CHF) that correspond to a transition from the nucleate boiling to film boiling regime, where almost the whole heater is covered by a thin film of vapor. Beyond the CHF a vapor layer is developed between the liquid and the surface acting like an insulator, rising abruptly the surface temperature, if the power is not cut immediately the surface may be melted (burn out). CHF is the main thermal performance limiter in nuclear reactors, forcing the power plant to operate in safety margins of heat flux. The enhancement of the CHF can increase the operational safety margin, leading in an increase of its efficiency. An increment of 32% in CHF could increase 20% in power generate in pressurized water reactor (Buongiorno et al., 2008).

Recently, nanostructured surfaces have attracted the attention because they may increase the CHF up to 100% (Forrest et al., 2010). Nanostructured surface can be obtained through pool boiling of nanofluids over a surface. The boiling process creates a nanoparticles coating. This layer affects the surface physical properties, changing the liquid-gas and solid surface tensions, the contact angle (Vafaei et al., 2006, 2011), as well as the surface roughness (Chopkar et al., 2008; Narayan et al., 2007; Kim et al., 2008).

In this context, the present work investigates how different materials and concentrations of nanoparticles deposited on a flat aluminum plate through the boiling process can affect the surface wettability and the surface roughness. The depositions of nanoparticles were obtained through pool boiling of nanofluids of water/Al_2O_3 of 20-30nm and 40-80nm for nanoparticles volumetric concentrations of 0.01%, 0.1% and 0.5%. Initial results demonstrated that the contact angle of surfaces covered with nanoparticles layer is near to zero. Due to the impossibility of evaluating the contact angle of superhidrophilic surfaces by usual methods, a new methodology was developed. This new approach is based on the spreading velocity of a water droplet deposited on the surface coated with nanoparticles. The aim of this study is to evaluate the wettability on the surfaces covered with nanoparticles through a new perspective that can be described as how fast a water droplet spreads through the surface, especially for the first milliseconds.

2. EXPERIMENTAL APARATUS AND PROCEDURE

2.1. Nanofluid preparation

The nanofluids were prepared according to the two-step method that consists on adding the desired amount of nanoparticles into a suitable host liquid (DI-water for the present work) and homogenizing the solution. Due to high surface energy, agglomeration and clustering are probable. To minimize this effect and promote a homogenous dispersion, an ultrasonic homogenizer (ColeParmer CP505) was applied. According to Weng and Ding (2005) the average size of agglomerates and clusters rapidly decreases during the first 50 minutes of sonication. However, Motta (2012) concluded that the probe of the agitation equipment can be damaged due to cavitation phenomenon and portion of it may also be dispersed into the nanofluid. In order to minimize this contamination, the agitation time adopted in the present work was 30 minutes, resulting in a stable solution with a minimum period of ultrasonication (Moraes, 2012)
Table 1 brings some characteristics of the nanoparticles purchased from Nanostructured & Amorphous Materials. The nanofluids were prepared for volumetric concentrations of 0.01%, 0.1% and 0.5%, using 300ml of DI-water as host fluid. The digital balance used to weight the nanoparticles was the Metler-Toledo AG245 with resolution of 0.0001g and the volume of DI-water was measured through a graduated cylinder. The error associated with each concentration is 0.33%

Table 1 - Nanoparticles characteristics

Nanoparticles	Average particle size (nm)	Density (g/cm^3)	Purity (%)	Specific surface area (m^2/g)	Morphology
$\gamma - Al_2O_3$	20-30	3.7	99.97	180	Nearly spherical
$\gamma - Al_2O_3$	40-80	3.7	99.00	100-200	Nearly spherical

2.2. Nanoparticle deposition

After ultrasonication, the nanofluid was transferred to the boiling system. The pool boiling procedure was set to 3 hours of boiling and it was performed in the apparatus shown in Fig.1, which possess a Schrader valve (1) responsible used to create vacuum and pressurize the system. The sphere valve (2) is responsible to fill or withdraw the nanofluid. Performing vacuum allows nanofluid to be inserted into the boiling system and pressurization facilitates the removal of nanofluid at final of each test. After the insertion of nanofluid, the bottom aluminum base (9) is heated by a cartridge resistance (10) of 245W, an aluminum plate (8), which is the plate where the boiling and deposition occur, a rubber disk (7) to seal all the bottom part, a flange (6) to accommodate a sealing ring (5) and borosilicate glass (4). The cooling aluminum block (3) is responsible to condense the water vapor, maintaining the amount of water during the boiling process. Cold water from a thermal bath is circulated through machined channels within the aluminum block (F). After each deposition, the sample was stored and the system was cleaned up with water and acetone for preparing a new sample. To prevent contamination of the deposited surfaces, all samples were stored into a glass container wrapped with aluminum foil.

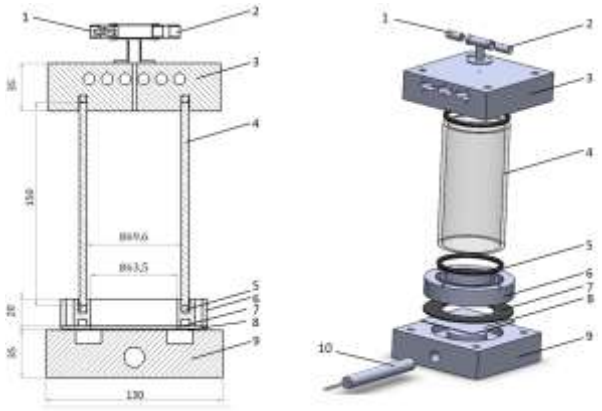

Figure 1 - The boiling apparatus (dimension are in millimeters).

Three samples covered for each type of nanoparticles were obtained after the deposition process, one for each nanofluid containing different nanoparticles concentrations. The deposited area is equal to 3167mm^2, corresponding to a circle with a diameter of 63.5mm. All samples were characterized according to their roughness and wettability.

2.3. Measurement of the surface roughness

Roughness measurements were performed using the equipment Veeco Wyko NT1100, providing 3D images of the surfaces with precision of 0.1 μm. The roughness was evaluated at five different positions of the samples and an

average roughness was stablished for each samples according to the parameters R_a (average roughness), R_q (root-mean-squared roughness), R_t (the highest peak-to-valley difference) and R_z (average of the ten greatest peak to valley).

2.4. Wettability evaluation

The new wettability evaluation method is based on the analysis of images obtained from a DI-water droplet spreading through a horizontal flat aluminum plate coated with nanoparticles. The obtained images that reveal the wetted area by the DI-water were analyzed through the software ImageJ V. 1.48. Figure 2 shows the apparatus developed to measure the wettability, which consists of a flat horizontal surface where the sample must be allocated, a light source, a high-speed camera (CamRecord 600) with lens AF MICRO NIKKOR 60mm and a micropipette. The camera was set to record images for 1s at 1000 frames per second with resolution of 1280x512 pixels. To ensure that the sample's surface was perpendicular to the camera, a digital inclinometer (DNM 60L Professional) with resolution of 0.1º was used. In order to obtain droplets with the same volume, an Eppendorf Research Plus micropipette was used, providing an error of 0.8%. The tests were performed for 8 µl because that was the maximum volume that remained steady in the pipette tip without being released by gravitational force. The droplet was released with a small hand perturbation on the opposite side of the pipette. In order to place the DI-water droplet in similar conditions on all surfaces, the distance between the surface and the needle tip was kept at 15mm.

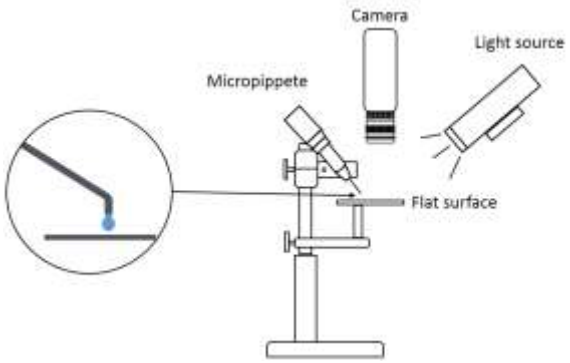

Figure 2 - Schematic of the experimental apparatus for wettability evaluation.

It was necessary to calibrate the image scale after setting up the apparatus in order to perform the tests. To calibrate the image scale is necessary to establish mm/pixel relation. A tape with known dimensions was placed on a flat aluminum surface with average width of 16.7 mm, corresponding to the average 517 pixels and resulting in a relation of 0.0323 mm/pixel.

After placing a DI-water droplet on the deposited surface and obtaining the images of the wetting process, each image was analyzed and the wetted area measured in the software ImageJ V. 1.48. Besides the wetted area, the contact line velocity could also be calculated. The image parameters could be adjusted for a better contrast of the wetted area against the dry area, however, due to the non-uniformity of the deposition and needle interference, a phase detection software was unable to identify the wetted area, then the areas were manually selected by the operator.

The method developed in the present study was validated by comparing the operator measurements against an image simulating the wetted area with known dimension. In order to verify if this method was capable of measuring precisely the area, the operator made 41 measurements. The results obtained are shown in Tab.2. To verify the significance of these results, t-student test with 95% confidence was applied in order to analyze if the area measured could be considered equal to the one expected. Statistically, it was concluded that the data acquired by the method does not require any correction.

Table 2 - Results of the area measured simulating wetted area

	Area (mm^2)	Standard deviation (mm^2)
Operator	33.068	0.082
Calculated	33.094	-

3. EXPERIMENTAL RESULTS AND DISCUSSION

3.1 Nanoparticles deposition

Figure 4 depict all obtained samples after the deposition of alumina 20-30nm and 40-80nm nanoparticles, respectively. These pictures evidence a visual non-uniformity of the nanoparticles' layers, except for alumina 0.01%

(20-30nm) and alumina 0.5% (40-80nm) covered samples. According to Vafaei and Borca-Tasciuc (2014), the deposition of nanoparticles occurs preferentially near the active nucleation sites, which may explain the non-uniformities of the surface. In addition, large deteriorated areas, characterized by regions apparently without covering layers, are identified in the samples produced by the boiling process of nanofluids containing 0.5% of alumina (20-30nm) nanoparticles. This deterioration of the deposited porous layer of nanoparticles can be related to a possible detachment of nanoparticles after the layer reaches a maximum thickness. This behavior was verified for different samples.

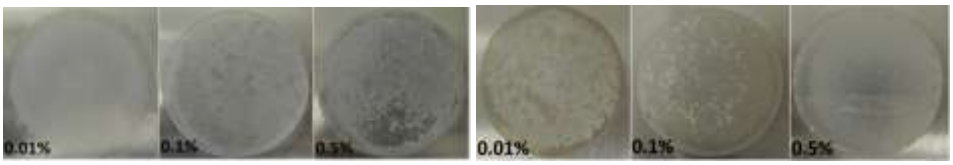

Figure 3 - The deposition of γ -Al_2O_3 20 – 30nm and 40-80nm respectively

3.2. Roughness results

Roughness of the samples was also measured, in order to identify the influence of the nanofluids concentration on the deposited porous layers. The profiles of the deteriorated regions were analyzed, corroborating the idea of a possible detachment of nanoparticles. The roughness of this sample was analyzed in different regions and compared to the roughness of the original aluminum plate. Table 3 presents roughness results of the deteriorated region of this sample, average values measured along the sample, and the results from the aluminum plate prior to the boiling process. From this table, it is possible to conclude that the roughness from the deteriorated region is more similar to the surface before boiling than to the non-deteriorated region, strengthening the hypothesis of the detachment of the nanoparticles porous layer.

Table 3 - Roughness for different regions of the same Al_2O_3 (20 – 30nm) 0.5% sample.

	Ra (nm)	Rq (nm)	Rz (μm)	Rt (μm)
Before boiling	570.76	711.39	4.17	4.47
Deteriorated region	827.27	1020	6.45	7.8
Sample	2030.0	2562.50	23.68	28.90

Roughness results of all samples are shown in Tab. 4, together with respective standard deviations. For the surfaces coated with γ-Al_2O_3 (20-30nm) nanoparticles the roughness seems to increase with rising volumetric concentration, while the opposite behavior is observed for the samples covered with γ-Al_2O_3 (40-80nm) nanoparticles. It should be noted, however, that the standard deviation also rises significantly with surface roughness, revealing the non-uniformity of the deposited layers over the surfaces coated with γ-Al_2O_3.

Table 4 - Roughness before and after the deposition of nanoparticles.

Sample	Concentration (%)	R_a (nm)	σ (nm)	R_q (nm)	σ (nm)	R_t (μm)	σ (μm)	R_z (μm)	σ (μm)
Before boiling	-	570.76	-	711.39	-	4.5	-	4.2	-
$\gamma - Al_2O_3\ (20-30nm)$	0.01	785.37	103.8	1017.3	147.7	17.8	2.1	13.1	2.7
$\gamma - Al_2O_3\ (20-30nm)$	0.1	1118.5	306.5	1482.0	423.9	20.6	5.7	16.5	4.0
$\gamma - Al_2O_3\ (20-30nm)$	0.5	2030.0	1081.3	2562.5	1322.3	28.9	5.2	23.7	4.1
$\gamma - Al_2O_3\ (40-80nm)$	0.01	2096.0	581.3	2726.0	719.7	35.9	9.5	29.2	6.8
$\gamma - Al_2O_3\ (40-80nm)$	0.1	1126.2	275.6	1642.0	465.7	27.5	5.7	24.0	6.3
$\gamma - Al_2O_3\ (40-80nm)$	0.5	975.7	142.3	1268.0	163.3	22.6	3.0	17.0	2.4

3.3. Evaluation of the wetted area

The static contact angle before the deposition of nanoparticle was 67.3° with 1.8° of standard deviation for 8μl of DI-water. As already described, the wettability of the samples was analyzed according to the spreading velocity of a water droplet deposited on the surface. Figure 4 illustrates the evolution of the wetted area during the first 10ms for the sample coated with Al_2O_3 for 0.1% of concentration in volume. During this period, the wetted area increased about 3.5 times. It is possible to observe that the wetted area presented a circular shape, and the apparent non-uniformities of this surface had no influence on the spreading behavior.

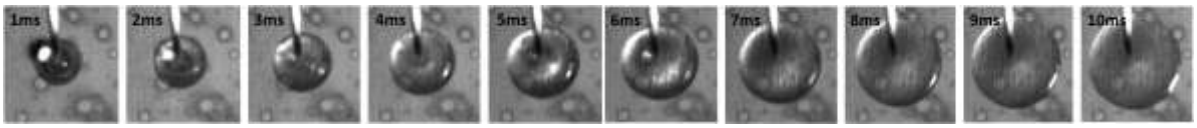

Figure 4 - Evolution of the wetted area for the sample coated with Al_2O_3 (20 – 30nm) for concentration of 0.1%. Frame rate of 1000 fps.

After the acquisition of the images of the spreading droplet on each sample, the evolution of the wetted area was evaluated. Figures 5 and 6 show this evolution for periods of 10ms and 1000ms for 8µl DI-water droplet right after the contact with the surface before the deposition of nanoparticles and the surfaces covered with γ-Al_2O_3 20-30nm and 40-80nm, respectively. The droplet quickly spread during the first 10ms, and then it continues to grow at a lower rate on most samples.

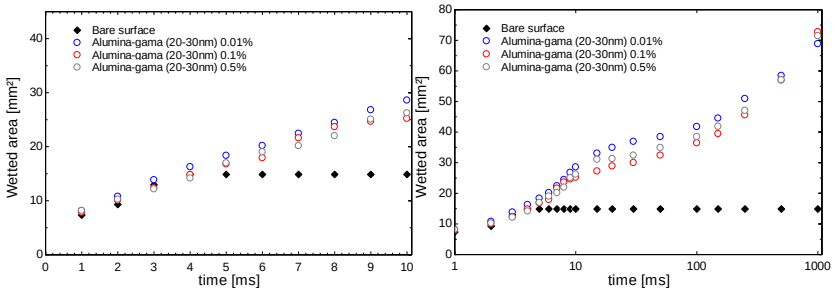

Figure 5 - Evolution of the wetted area for the surfaces coated with $\gamma - Al_2O_3$ (20 – 30nm)

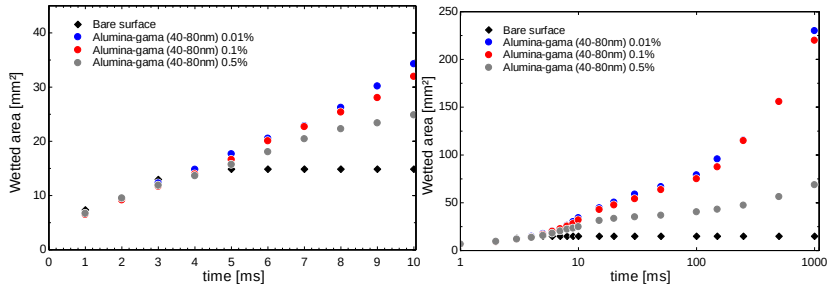

Figure 6 - Evolution of the wetted area for the surfaces coated with $\gamma - Al_2O_3$ (40 – 80nm)

For the surfaces coated with Al_2O_3 20-30nm, seen in Fig. 5, it is possible to notice that spreading velocity does not depend on the concentration. Nevertheless, for the surfaces coated with Al_2O_3 40-80nm nanoparticles the evolution wetted area is nearly the same for the 0.01% and 0.1% concentration, however the surfaces covered with 0.5% shows lower spreading velocity. It´s possible to notice that the spreading velocity is nearly the same for the first 4ms before and after the deposition of nanoparticles. These results may indicate a change of mechanisms actuating in the spreading behavior, probably governed by inertial effects due to the impact of the droplet on the surface during the first 4 milisseconds and then by capillarity effects due to the porous layer. The average spreading velocity of the contact line was calculated considering the radius variation of circles with areas equal to the measured wetted areas. In addition, due to the heterogeneous depositions of nanoparticles, the average spreading velocities in eight different directions of the contact line were calculated for the first 10ms. Each contact line symmetrically separated by 45 degrees.

Table 5 shows the calculated spreading velocities of the contact line of the water droplet in eight different directions and the average velocity, based on the measured area for all samples during the first 10ms. According to these results, it is possible to analyze the homogeneity of the spreading droplet and possible influences of surface inhomogeneity in the wetting behavior. The error associated with the calculated velocities of the contact line is $\pm$0.02mm/ms

Table 5 - Average spreading velocity of the border of the water droplet for the first 10ms.

Sample	V. C. (%)	$\overline{V_1}$ mm/ms	$\overline{V_2}$ mm/ms	$\overline{V_3}$ mm/ms	$\overline{V_4}$ mm/ms	$\overline{V_5}$ mm/ms	$\overline{V_6}$ mm/ms	$\overline{V_7}$ mm/ms	$\overline{V_8}$ mm/ms	$\overline{V}$ mm/ms	σ mm/ms
$\gamma - Al_2O_3$ (20 – 30nm)	0.01	0.312	0.301	0.276	0.299	0.307	0.267	0.294	0.295	0.294	0.15
$\gamma - Al_2O_3$ (20 – 30nm)	0.1	0.290	0.277	0.275	0.287	0.287	0.287	0.284	0.286	0.284	0.05
$\gamma - Al_2O_3$ (20 – 30nm)	0.5	0.284	0.291	0.289	0.297	0.291	0.286	0.283	0.286	0.288	0.04
$\gamma - Al_2O_3$ (40 – 80nm)	0.01	0.326	0.333	0.317	0.347	0.326	0.308	0.336	0.333	0.328	0.12
$\gamma - Al_2O_3$ (40 – 80nm)	0.1	0.320	0.320	0.329	0.320	0.317	0.313	0.317	0.320	0.319	0.04
$\gamma - Al_2O_3$ (40 – 80nm)	0.5	0.270	0.279	0.283	0.270	0.281	0.297	0.292	0.265	0.280	0.11

Visual observations of the shape of the water droplet spreading along the surfaces coated with aluminum oxide 20-30nm and 40-80nm for all concentrations showed nearly circular spreading droplets. This behavior can be confirmed by the calculated contact line velocities, which are similar for the eight directions. The roughness inhomogeneity of the samples not promoted a preferential spreading direction. It can be speculated that the capillarity has a dominant effect over the roughness.

4. CONCLUSIONS

This study demonstrates that pool boiling of nanofluids has a great potential to modify the properties of heated surfaces due to the deposition of nanoparticles, consequently creating porous layers that modify the surfaces' wettability. Due to the impossibility to measure contact angles close to zero by conventional methods, a new method was developed based on the spreading velocity of a DI-water droplet along the surface. The main findings of this study are summarized as follows:

- The deposition of nanoparticles on a surface through pool boiling of nanofluids made the surfaces super-wetting independently of the employed nanoparticles and of its concentrations during the boiled process;
- Surface roughness of the samples have increased with the deposition of nanoparticles.
- Two mechanisms were identified for the observed spreading behavior, with inertial effects governing during the first 4 milliseconds and capillarity effects acting to further spread the droplets.
- The spreading velocity is nearly the same for the first 10 milliseconds for the surfaces covered with $\gamma - Al_2O_3$. At the final of the 1 second the wetted area of the surfaces covered with $\gamma - Al_2O_3\ (40 - 80nm)$ for 0.01% and 0.1% are 3 times bigger than the surfaces covered with $\gamma - Al_2O_3\ (20 - 30nm)$ and $\gamma - Al_2O_3\ (40 - 80nm)$ 0.5%.

5. ACKNOWLEDGEMENTS

The authors gratefully acknowledge the financial support provided by NANOBIOTEC-CAPES, FAPESP (2011/13119-0) and CNPq (404437/2015-0). The support given to this investigation by Prof. Dr. Renato Goulart Jasinevicius and Hélio Donisetti Trebi is also appreciated and deeply recognized.

6. REFERENCES

BUONGIORNO, J.; HU, L. W.; KIM, S. J; HANNINK, R.; TRUONG, B.; FORREST, E. Nanofluids for enhanced economics and safety of nuclear reactors: an evaluation of the potential features, issues, and research gaps. Nuclear Technology. v. 162, p. 80–91, 2008.

CHOPKAR, M.; DAS, A. K.; MANNA, I.; DAS, P. K. Pool boiling heat transfer characteristics of ZrO2–water nanofluids from a flat surface in a pool. Heat and Mass Transfer, v. 44, n. 8, p. 999–1004, 2008.

KIM, S. J.; MCKRELL, T.; BUONGIORNO, J.; HU, L. Alumina Nanoparticles Enhance the Flow Boiling Critical Heat Flux of Water at Low Pressure. v. 130, n. April, p. 18–20, 2008.

MORAES, A. A. U. Avaliação teórica e experimental do coeficiente de transferência de calor e do fluxo crítico durante ebulição convectiva de nanofluidos. Relatório final de Pós-Doutorado. Escola de Engenharia de São Carlos. Universidade de São Paulo. São Carlos. 2012.

MOTTA, F. C. Caracterização da condutividade térmica, viscosidade dinâmica e ângulo de contato de nanofluidos baseados em particulas de alumina-gama em água. Dissertação de Mestrado. Escola de Engenharia de São Carlos. Universidade de São Paulo. São Carlos. 2012.

NARAYAN, G. P.; ANOOP, K. B.; DAS, S. K. Mechanism of enhancement / deterioration of boiling heat transfer using stable nanoparticle suspensions over vertical tubes. Journal of Applied Physics, v. 074317, n. 2007, 2015.

VAFAEI, S.; BORCA-TASCIUC, T.; PODOWSKI, M. Z.; PURKAYASTHA, A. .; RAMANATH, G.; AJAYAN, P. M. Effect of nanoparticles on sessile droplet contact angle. Nanotechnology, v. 17, p. 2523–2527, 2006.

VAFAEI, S.; WEN, D. Flow boiling heat transfer of alumina nanofluids in single microchannels and the roles of nanoparticles. Journal Nanopart Res. v. 13, p. 1063–1073, 2011.

VAFAEI, S., BORCA-TASCIUC, T. Role of nanoparticles on nanofluid boiling phenomenon: Nanoparticle deposition. Chemical Engineering Research and Design v. 92, p. 842–586, 2014.

WEN, D.; DING, Y. Formulation of nanofluids for natural convective heat transfer applications. International Journal of Heat and Fluid Flow, v. 26, n. 6, p. 855–864, 2005.

7. RESPONSIBILITY NOTICE

The authors are the only responsible for the printed material included in this paper.